American Journal of Pathology, Vol. 167, No. 4, October 2005

Immunopathology and Infectious Diseases

Apoptosis of Hepatocytes Caused by Punta Toro Virus (*Bunyaviridae: Phlebovirus*) and Its Implication for Phlebovirus Pathogenesis

Xiaohua Ding,* Fangling Xu,* Hongli Chen,* Robert B. Tesh,*‡ and Shu-Yuan Xiao*‡§

From the Departments of Pathology and Internal Medicine,§ and the Institute of Human Infections and Immunity,‡ University of Texas Medical Branch, Galveston, Texas*

Experimental infection of hamsters with Punta Toro virus (PTV) produces a disease with clinical and pathological similarities to the severe human hemorrhagic fever caused by Rift Valley fever virus (RVFV), thus providing an animal model for RVFV pathogenesis. In this model, hepatocytic apoptosis is the main pathological component of liver injuries that are responsible for severe hemorrhagic manifestations. To further elucidate whether viral replication in hepatocytes directly causes apoptosis, we studied the morphological and biochemical changes of apoptosis in HepG2 cells at different time points after PTV infection. Cellular viability began to decrease 12 hours after infection compared with controls. Caspases 3/7 were activated significantly at 48 and 72 hours after infection, and phosphatidylserine translocation and DNA fragmentation were also detected at 48 and 72 hours. Cell cycle analysis by flow cytometry showed that infected HepG2 cells were arrested at G_0/G_1 phase. Furthermore, virus titer increased with apoptosis progression, suggesting that viral replication is necessary for the apoptotic process. These results indicate that PTV infection alone, without a secondary inflammatory cellular reaction, induces hepatocytic apoptosis and suggest that future therapeutics for RVFV hemorrhagic disease might target inhibition of cellular apoptotic pathways during the acute infection. ***(Am J Pathol 2005, 167:1043–1049)***

Punta Toro virus (PTV) is a member of the genus *Phlebovirus*, family *Bunyaviridae*. Viruses in this genus contain a negative-sense, single-strand RNA genome that consists of three segments, large (L), medium (M), and small (S), and are associated with a variety of diseases, including a brief self-limited febrile illness, retinitis, encephalitis, meningoencephalitis, and a severe hemorrhagic fever.[1,2] The most important member of the Phlebovirus genus is Rift Valley fever virus (RVFV), which is a significant veterinary and human pathogen in sub-Saharan Africa. Occasionally, RVFV has also caused epidemics/epizootics outside of the endemic region, as illustrated by recent outbreaks in Africa and the Middle East.[3–6] Because of its epidemic potential and transmissibility, RVFV is considered a potential bioterrorist threat. The pathogenesis of RVFV is poorly understood, in part because it is classified as a biosafety level-4 (BSL-4) agent, and few laboratories have the maximum containment facilities necessary to handle it.

Recently, we described a hamster model of hemorrhagic fever caused by PTV, which has many similarities to the severe disease produced in animals and humans by RVFV. One of the main pathological findings in the PTV hamster model was the brisk apoptosis of hepatocytes associated with the acute illness.[7] Cusi et al[8] also found that Toscana virus, another member of *Phlebovirus*, induced apoptotic death of infected neurons in a mouse model. The hepatic pathology seen may in part explain the fulminant liver injury seen in humans and animals infected by RVFV.[9] To elucidate the pathogenesis of phlebovirus-induced liver injury, one question that needs to be addressed is whether virus infection alone induced apoptosis or whether other host factors such as an inflammatory cellular response are required. Therefore, the purpose of this *in vitro* study was to examine whether PTV infection in a pure cell population can result in apoptosis.

Supported by National Institutes of Health contract N01-AI-25489.

Accepted for publication June 30, 2005.

Current address of X.D.: Virus Research Institute, Wuhan University Medical College, Wuhan, Hubei Province, Peoples' Republic of China.

Address reprint requests to Shu-Yuan Xiao, M.D., Department of Pathology, University of Texas Medical Branch, 301 University Blvd., Galveston, TX 77555-0588. E-mail: syxiao@utmb.edu.

Materials and Methods

Virus and Cell Line Used

The Adames and Balliet strains of PTV were used in this study. Both virus strains were isolated from febrile patients in Panama[10,11] and had been passaged 12 times in baby mice and 3 times in Vero cells. The titers for PTV Adames and Balliet were 5×10^6 and 3.25×10^7 plaque forming units PFU/ml, respectively. The HepG2/C3A clone of human hepatoblastoma cells was used as the virus substrate and was obtained from the American Type Culture Collection (Rockville, MD). Cells were grown at 37°C in modified Eagle's minimum essential medium (MEM), supplemented with 10% fetal bovine serum, 0.29 mg/ml L-glutamine, 100 U/ml penicillin G, and 100 μg/ml streptomycin sulfate.

Infection of Cells and Virus Titration

HepG2 cells were infected with PTV at a multiplicity of infection of 3~5 throughout the study. Minimum essential medium supplemented with 2% fetal bovine serum was added after 2 hours of absorption for maintenance. Cells were harvested at different time points postinfection (p.i.) (see below) for cellular viability, caspase 3/7, phosphatidylserine, DNA fragmentation, Bcl-2 and Bax gene expression, and cell cycle analyses. Virus proliferation was assayed by plaque assay[7] in Vero cells inoculated with culture medium taken from HepG2 cells infected with the viruses at 0, 12, 24, 48, and 72 hours p.i.

Tetrazolium Salt Thiazolyl Blue Assay

PTV was inoculated into 96-well plates seeded with HepG2 cells when the cells reached confluency. At 0, 12, 24, 48, and 72 hours p.i., 100 μl of the medium was removed and replaced with an equal volume of fresh medium containing 5 mg/ml of the tetrazolium salt thiazolyl blue (MTT; Sigma). Plates were incubated at 37°C under 5% CO_2 for 4 hours. After careful aspiration of the medium, 100 μl of dimethyl sulfoxide was added to each well, and plates were shaken at room temperature for 10 minutes. Cellular viability was determined by measuring the absorbance at 570 nm by spectroscopy (reference wavelength 690 nm). All experiments were performed in triplicate.

Caspase 3/7 in Situ *Assay*

For each test, 10^4 to 10^5 per well of HepG2 cells was grown in 8-well chamber slides (Nalge Nunc International, Rochester, NY). When the cell monolayer was nearly confluent, PTV was inoculated as indicated. At 0, 12, 24, 48, and 72 hours p.i., caspases were detected in living cells according to the protocol of the CaspaTag *in situ* apoptosis detection kit (Chemicon, Temecula, CA). First, freshly prepared 30× fluorochrome inhibitors of caspases reagent solution at a 1:30 dilution in culture medium was added and mixed well. After incubation for 1 hour at 37°C in 5% CO_2, the medium was discarded, and Hoechst stain (0.5% v/v) was added and incubated for 5 minutes at 37°C. After two washes with 2 ml of 1× wash buffer, the plastic divider was removed; a drop of diluted fixative (1:10 with wash buffer) was added; and a coverslip was applied. Cells were examined under a fluorescence microscope for green fluorescence and nuclear staining of caspase-positive cells. Ten 40× microscope fields were observed to determine the number of positive cells.

Annexin V-Flourescein Staining

HepG2 cells grown in 8-well chamber slides were inoculated with the virus as described. At 0, 12, 24, 48, and 72 hours p.i., the supernatant was discarded, and cells were washed with phosphate-buffered saline (PBS). After removing the plastic divider, 50 μl of staining solution (Roche Diagnostic, Indianapolis, IN) containing annexin V-fluorescein and propidium iodide was added to each well with a coverslip and incubated for 15 minutes at 22°C. Then cells were examined under a fluorescence microscope.

Terminal Deoxynucleotidyl Transferase-Mediated dUTP Nick End-Labeling Assay

HepG2 cells were grown in 8-well chamber slides (Nalge Nunc International). When the cells had reached 90% confluence, PTV was added. At 0, 12, 24, 48, and 72 hours p.i., the plastic divider was removed from the chamber slide, and the cells were fixed in 1% paraformaldehyde in PBS (pH 7.4) in a coplin jar for 10 minutes at room temperature, washed twice in PBS, and postfixed in precooled ethanol:acetic acid (2:1 v/v) for 5 minutes. After two final washes in PBS, excess liquid was carefully removed. Then 75 μl of equilibration buffer was added directly to the specimen. After gently tapping off excess liquid and carefully blotting around the section, terminal deoxynucleotidyl transferase-mediated UTP nick-end labeling (TUNEL) reaction mixture (Serologicals Corp., Norcross, GA) containing fluorescein isothiocyanate-labeled dUTP and terminal deoxynucleotidyl transferase was added immediately, followed by incubation at 37°C for 1 hour in a moist dark chamber. The specimen was transferred to a coplin jar containing working strength stop/wash buffer and incubated for 10 minutes at room temperature after it was agitated for 15 seconds. Excess liquid was carefully removed, and mounting medium containing 0.5 to 1.0 μg/ml propidium iodide was added. The slide was covered with a glass coverslip, and the stained cells were viewed under a fluorescent microscope, using standard fluorescein excitation and emission filters.

Cell Cycle Analysis

At 0, 12, 24, 48, and 72 hours p.i., 2 to 3×10^6 cells were harvested according to the DNA staining technique[12] in triplicate. Trypsinized cells were washed once with cold

PBS/0.1% azide solution and resuspended in 1 ml of low-salt stain [4 mmol/L sodium citrate, 3% polyethylene glycol 8000, 1 mg/ml propidium iodide (Sigma), 180 U/ml RNase A(Worthington Biochemicals), and 1% Triton X-100 in PBS/azide] in a 15-ml centrifuge tubes by gently vortexing. Tubes were put in 37°C water bath for 20 minutes with gentle mixing every 5 minutes while covered with aluminum foil to protect them from light. Then 1 ml of high-salt stain [400 mmol/L sodium chloride, 3% polyethylene glycol 8000, 1 mg/ml propidium iodide (Sigma), and 1% Triton X-100 in PBS/azide] was added by gently vortexing and stored at 4°C overnight. Then cells were analyzed by flow cytometry (BD Biosciences) in the flow cytometry and cell sorting core laboratory, with 10,000 events collected from each sample.

RNA Extraction, cDNA Synthesis, and Real-Time Polymerase Chain Reaction (PCR) Analysis

At 0, 3, 6, and 12 hours p.i., total RNA preparations from 10^6 Balliet strain-infected and uninfected cells were obtained by the guanidine isothiocyanate method, using Trizol (Gibco-BRL, Grand Island, NY) according to the manufacturer's instruction. Potential contamination by cellular DNA was prevented by treating the extract with DNase I. To assess mRNA expression, a reverse transcription-polymerase chain reaction was used. For the RT reaction, total RNA was primed with hexanucleotide random primers and reverse-transcribed with SuperScript II reverse transcriptase (Gibco-BRL) in a 20-μl reaction. The newly synthesized cDNA was subjected to amplification using the IQTM SYBR Green Supermix (Bio-Rad) for real-time PCR, following the manufacturer's instructions. Amplification was performed in a 25-μl reaction mixture containing 1× SYBR Green mix, 5 pmol each of forward and reverse primers, 3.5 mmol/L $MgCl_2$, and 2 μl of target cDNA. The β-actin gene was used as an internal control. The PCR products were 210, 160, and 229 bp long for the Bcl-2, bax, and β-actin genes, respectively. Conditions for cycling were 95°C for 3 minutes, followed by 35 cycles of denaturation at 95°C for 20 seconds; annealing at 47°C for 20 seconds for bax and β-actin; 67°C for 20 seconds for bcl-2 gene; extension at 72°C for 30 seconds; and fluorescence reading at 82°C for 30 seconds. Amplification and detection were performed with the Smart Cycler (Cepheid, Sunnyvale, CA). A negative control was included in each run, and the specificity of amplification reaction was checked by melting curve analysis.

Statistical Analysis

The DNA content of the cells, as assayed using a fluorescence-activated cell sorter, was analyzed using ModFit LT version 2.0. Cepheid Smart Cycle Version 2.0b was used to analyze the raw data of real time PCR. Experimentally determined standard curves were, in turn, used to estimate the concentration of each sample. For other parameters, SPSS 12.0 was used to analyze pairwise comparisons by the independent samples *t*-test and Wilcoxon rank sum test. A *P* value of less than 0.05 was considered statistically significant.

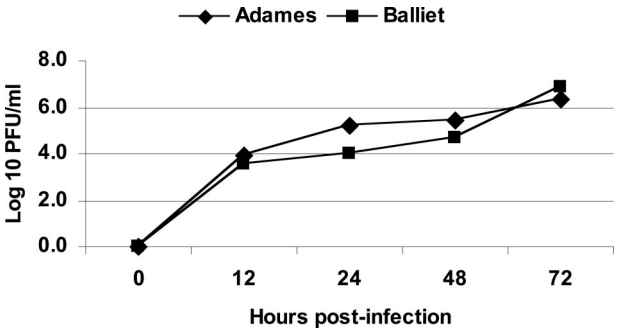

Figure 1. Growth curves of the Adames and Balliet strains of PTV in HepG2 cells (means of duplicate).

Results

PTV Titration

The level of virus replication was measured from the culture medium at different time points by plaque assay. As shown in Figure 1, both strains of PTV proliferated rapidly after infection, but the rate of proliferation decreased from 12 to 48 hours p.i. Replication was slightly slower for the Balliet strain than the Adames strain from 12 to 48 hours p.i. This pattern was inverted at 72 hours p.i.

Changes in Viability of HepG2 Cells Infected with PTV

The HepG2 cells infected with PTV appeared normal in morphology and did not exhibit evident viral cytopathic effect (CPE) until 2 days p.i. Cellular adherence decreased gradually 2 days p.i. At day 3, many cells were rounded up and had detached from the flask wall (Figure 2A). The proliferation of HepG2 cells was analyzed by MTT assay (Figure 2B). It showed that viability of Balliet-infected HepG2 cells started to decrease after infection and reduced significantly ($P < 0.05$) at 12 ($P = 0.047$), 24 ($P = 0.002$), and 72 hours ($P = 0.003$) p.i. compared with the uninfected cells. For Adames-infected cells, viability was reduced at 24 ($P = 0.001$) and 72 hours ($P = 0.030$) p.i. There was no evident difference at 0 and 48 hours p.i.

Activities of Caspases

As shown in Figure 3, A and B, caspase 3/7 activation began at 12 hours p.i., and the change of activity level was significant ($P < 0.05$) at 24, 48, and 72 hours p.i. Caspase activity was similar in Adames-infected and the Balliet-infected cells at 24 and 48 hours p.i., but higher in the Balliet-infected cells at 72 hours p.i. (Figure 3B).

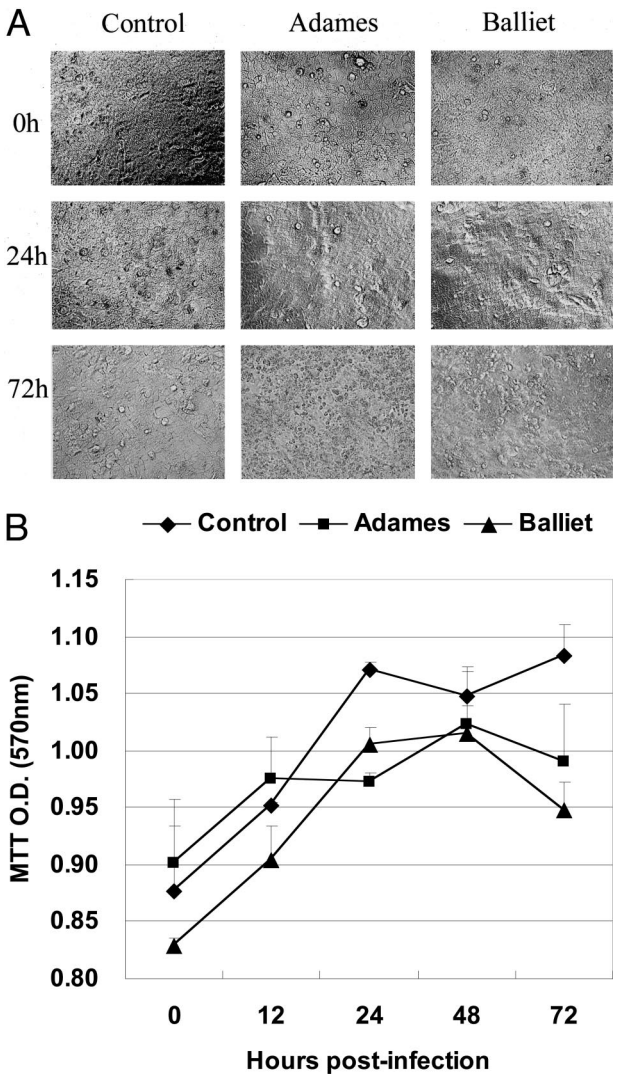

Figure 2. CPE associated with replication of PTV in HepG2 cells. **A:** Morphological appearance for HepG2 cells with PTV infection at 0, 24, and 72 hours p.i. (40× objective). Many infected cells have rounded up and detached from the wall of plate. **B:** Viability of HepG2 cells as determined by MTT assay (mean ± SD).

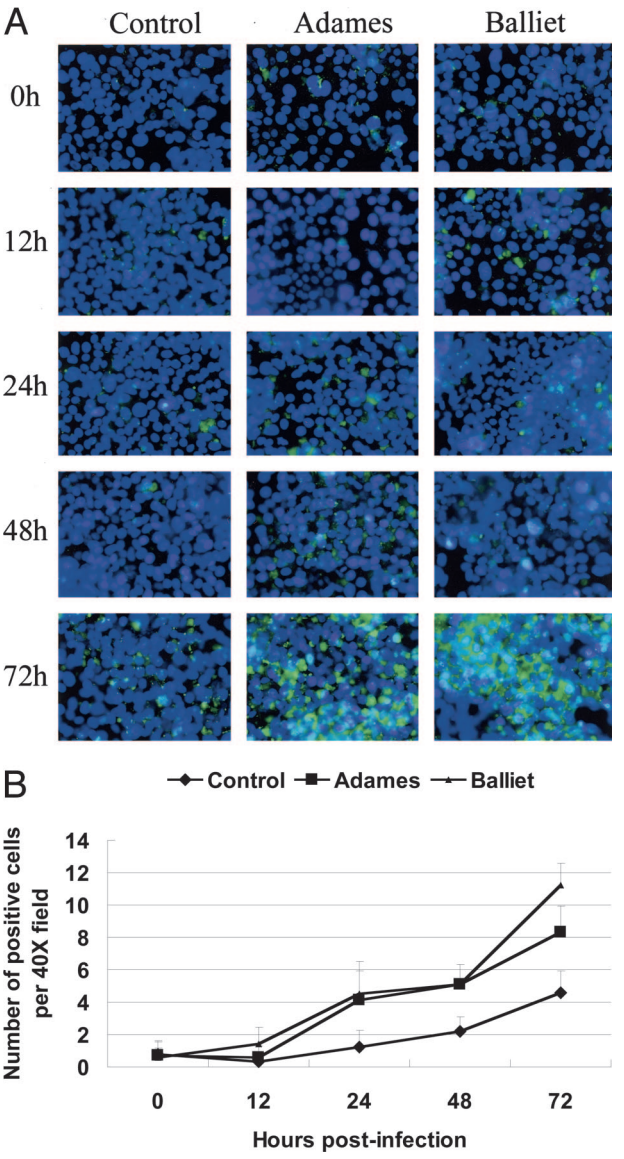

Figure 3. Activities of caspases. **A:** Casapase 3/7-positive staining cells (40× objective). Bright blue fluorescence of nuclei corresponds to caspase 3/7-positive staining cells. **B:** Number of positive HepG2 cells at different time points in *in situ* analysis (mean ± SD).

Phosphatidylserine Translocation

Another manifestation of apoptosis, the relocation of phosphatidylserine to the cell membrane, was detected by annexin V staining. There was no apparent change before 24 hours p.i. The number of annexin V-positive cells was significantly elevated in Balliet-infected cells ($P < 0.05$). Annexin V-positive cells were also increased in Adames-infected cells at 48 and 72 hours p.i., but lower than the Balliet strain (Figure 4).

DNA Fragmentation

In situ TUNEL was used to examine for DNA fragmentation in HepG2 cells. Bright green spots representing nuclei of apoptotic cells were evident in the infected cells at 48 and 72 hours p.i. ($P < 0.05$) but were scarcely seen in the uninfected control cells (Figure 5A). Furthermore, DNA fragmentation increased with the progression of infection (Figure 5B).

Cell Cycle Analysis

The state of cell growth was assayed using a fluorescence-activated cell sorter for cell cycle of the infected HepG2 cells. As shown in Figure 6, the Balliet-infected cells at G_0/G_1 (91.48%; Figure 6A) and sub-G_1 (3.19%; Figure 6D) phases significantly ($P < 0.05$) increased, and cells at G_2/M phase (5.36%; Figure 6C) decreased at 72 hours p.i. Adames-infected cells had the highest level in G_0/G_1 phase and the lowest level in G_2/M phase at 48 hours p.i., and significant decreases of Adames-infected cells at S phase were seen at 12 and 24 hours p.i. ($P < 0.05$) (Figure 6B).

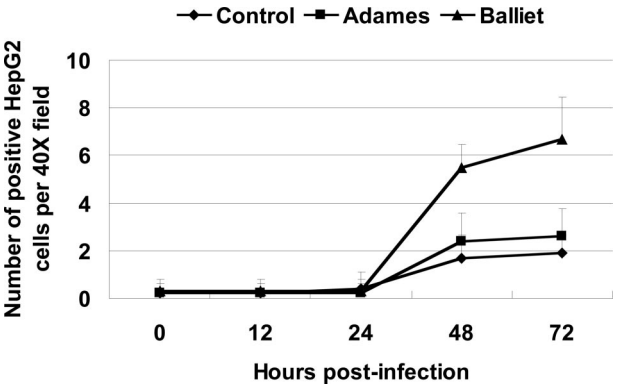

Figure 4. PS translocation assay. Number of apoptotic cells stained with annexin V-FLUOS in PTV-infected and noninfected (control) HepG2 cells (mean ± SD).

Expression of Bcl-2 and Bax Genes

Expressions of Bcl-2 and Bax genes were examined by real-time PCR in Balliet-infected cells. As shown in Figure 7A, expression of Bcl-2 was lower in infected cells than in uninfected control, at 6 and 12 hours p.i. In contrast, expression of Bax was higher in infected cells at 6 and 12 hours, especially at 12 hours p.i. (Figure 7B). As a control, the level of β-actin mRNA remained unchanged throughout the course of the experiment.

Discussion

Recent success in developing a hamster model of PTV provides an opportunity to study the pathogenesis of severe phlebovirus disease. Hepatocytic apoptosis constituted the main mechanism of severe liver injury in the hamster model.[7] One of the questions derived from that study was whether viral invasion and replication in hepatocytes was directly responsible for this pathological process or was apoptosis the result of a secondary inflammatory cellular infiltration? There are no other studies in literature that focused on this issue. Recently, the study of a mouse model reported that Toscana virus infection in the central nervous system induced neuronal apoptosis and that it was closely related to acute encephalitis and death of mice.[8] Studies on members of another genus (*Hantavirus*) of the family (*Bunyaviridae*) indicate that hantaviruses induce apoptosis *in vitro*.[13–18] To specifically address this question with phleboviruses, an *in vitro* study using a single-cell population, a hepatic cell line of human origin, was conducted.

A large number of RNA and DNA viruses can induce apoptosis, both in cell culture and *in vivo*, and apoptosis is a common consequence of virus replication.[19,20] Viral gene products can modulate apoptosis, positively or negatively. Induction of apoptosis contributes directly to the cytopathic effects of many viruses. Suppression of apoptosis, however, may prevent premature death of infected cells, thereby facilitating viral replication, spread, or persistence.[13,21,22]

Caspase 3 (CPP32) activation, translocation of phosphatidyl serine (PS), and DNA fragmentation are markers

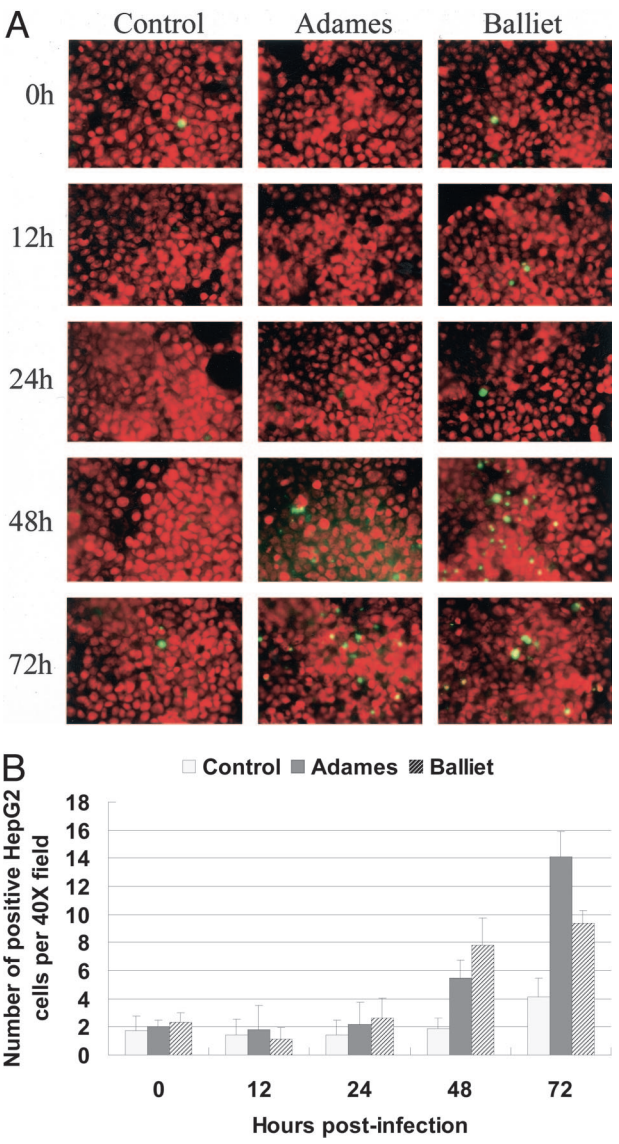

Figure 5. DNA fragmentation analysis. **A:** TUNEL analysis of Punta Toro virus-infected HepG2 cells (40× objective). Green nuclear fluorescence correspond to positive staining. **B:** Number of apoptotic cells stained with fluorescein isothiocyanate and propidium iodide in control and PTV-infected HepG2 cells (mean ± SD).

of the early and late phases of apoptosis.[19,23] In this study, we detected the activities of caspase 3/7, phosphatidylserine translocation, DNA fragmentation, and DNA content of HepG2 cells infected with PTV Adames and Balliet strains at different time points after infection. It showed a correlation between the reduction of cell viability and the virus replication (Figures 1 and 2). There was an increase in measurable caspase 3/7 activity occurring at 24 hours p.i. (Figure 3A), which became more prominent at 48 and 72 hours p.i. (Figure 3B). As the effector caspases, active caspase 3, 6, and 7 are responsible for the cleavage of a broad array of cellular targets,[24] leading to the further disassembly of cell structure.[25] As evidenced by positive annexin V staining (Figure 4) and DNA fragmentation (Figure 5), these biochemical changes resulted in morphological changes of

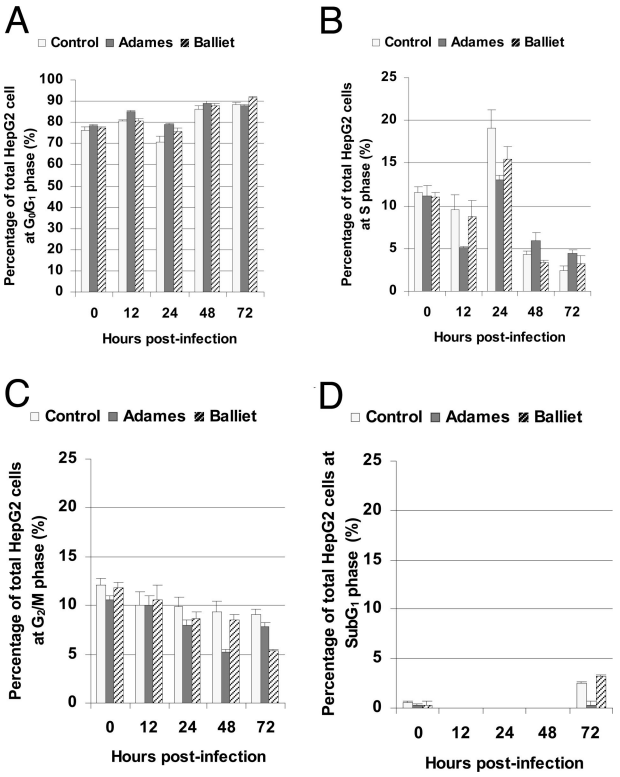

Figure 6. Percentage (ratio ± SD%) of HepG2 in various cell cycle phases at different time points. DNA content was detected by flow cytometry after propidium iodide staining. **A:** Percentage of total HepG2 at G_0/G_1 phases. **B:** Percentage of total HepG2 at S phases. **C:** Percentage of total HepG2 at G_2/M phases. **D:** Percentage of total HepG2 at sub-G_1 phases.

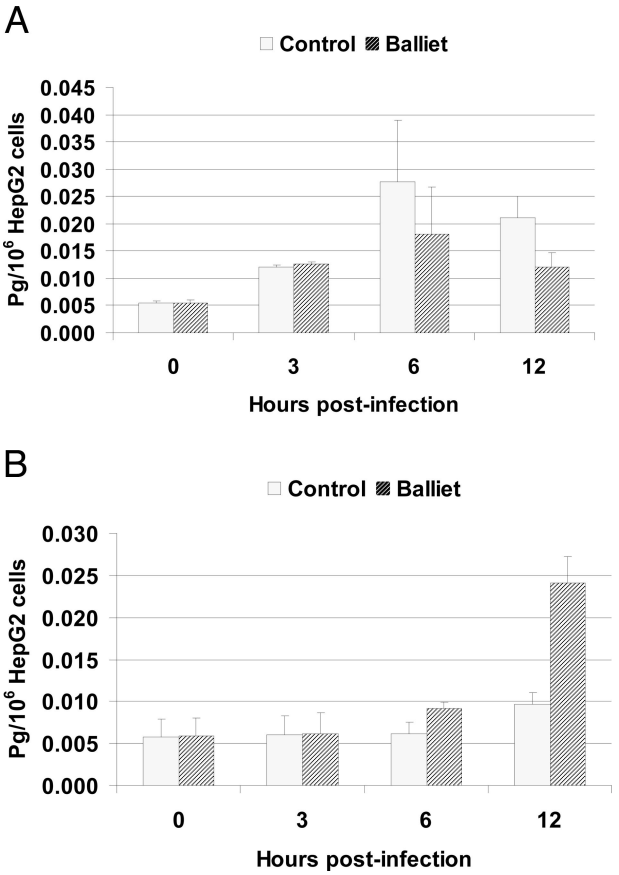

Figure 7. Analysis of gene expression of Balliet strain-infected and noninfected HepG2 cells (mean ± SD). **A:** Bcl-2 gene. **B:** Bax gene.

apoptosis, particularly at 48 and 72 hours p.i. The cell cycle analysis (Figure 6) showed G_0/G_1 arrest and apoptosis at 72 hours p.i., confirming the results of MTT assay, which showed decrease in viability in the infected cells (Figure 2). All of these indicate that PTV can block HepG2 cell proliferation in G_0/G_1 phase, and the apoptosis might be the mechanism of CPE in PTV-infected HepG2 cells. At 48 and 72 hours p.i., HepG2 cells infected with Balliet strain presented more significant variations of early apoptotic markers: caspase activation and PS translocation (Figures 3 and 4), whereas for DNA fragmentation, the late apoptotic marker, Adames-infected cells showed higher effects. This suggests that apoptosis developed more quickly in Adames-infected cells than in Balliet-infected cells. Gene expression analysis of the Bcl-2 gene family, which encodes antiapoptotic or proapoptotic proteins and plays an important role in both up and down-regulation of apoptosis,[26,27] showed that the expression of the proapoptotic B*ax* gene increased and antiapoptotic Bcl-2 gene decreased at 12 hours p.i. (Figure 7), indicating involvement of the mitochondria pathway. Interestingly, these may be related to the mitochondrial dysfunction as measured by the MTT assay (Figure 2B).[28]

The findings of both morphological and biochemical characteristics of apoptosis in PTV-induced HepG2 cells indicate that apoptotic cell death is a main pathogenic component in phlebovirus infection. To our knowledge, this is the first study demonstrating that a phlebovirus directly induces target cell apoptosis and that this process is associated with an imbalance of mitochondrial function. And a low but significant degree of genetic divergence between Adames and Balliet viruses may be responsible for the subtle differences observed in the individual apoptosis markers. Further studies need to be done to gain insight into the mechanism by which PTV with different virulence in hamster induces apoptosis in HepG2 cells and to elucidate the pathogenesis of phlebovirus-associated disease.

Acknowledgments

We thank Mengyi Ye and Hilda Guzman for technical assistance.

References

1. Tesh RB: The Genus *Phlebovirus* and its vectors. Annu Rev Entomol 1988, 33:169–181
2. Nichol ST: Bunyaviruses. Fields Virology, vol 2. Edited by Knipe DM, Howley PM, Griffin DE, Lamb RA, Martin MA, Roizman B, Straus SE. Philadelphia, Lippincott Williams & Wilkins, 2001, 1603–1633
3. Tetsuro I, Shinji M: Rift Valley fever virus. Uirusu 2004, 54:229–235
4. Woods CW, Karpati AM, Grein T, McCarthy N, Gaturuku P, Muchiri E, Dunster L, Henderson A, Khan AS, Swanepoel R, Bonmarin I, Martin L, Mann P, Smoak BL, Ryan M, Ksiazek TG, Arthur RR, Ndikuyeze A, Agata NN, Peters CJ, World Health Organization Hemorrhagic Fever

Task Force: An outbreak of Rift Valley fever in Northeastern Kenya, 1997–98. Emerg Infect Dis 2002, 8:138–144
5. Morvan J, Saluzzo JF, Fontenille D, Rollin PE, Coulanges P: Rift Valley fever on the east coast of Madagascar. Res Virol 1991, 142:475–482
6. Shoemaker T, Boulianne C, Vincent MJ, Pezzanite L, Al-Qahtani MM, Al-Mazrou Y, Khan AS, Rollin PE, Swanepoel R, Ksiazek TG, Nichol ST: Genetic analysis of viruses associated with emergence of Rift Valley fever in Saudi Arabia and Yemen, 2000–01. Emerg Infect Dis 2002, 8:1415–1420
7. Fisher AF, Tesh RB, Tonry J, Guzman H, Liu D, Xiao SY: Induction of severe disease in hamsters by two sandfly fever group viruses, Punta Toro and Gabek Forest (Phlebovirus; Bunyaviridae), similar to that caused by Rift Valley fever virus. Am J Trop Med Hyg 2003, 69:269–276
8. Cusi MG, Gori Savellini G, Terrosi C, Di Genova G, Valassina M, Valentini M, Bartolommei S, Miracco C: Development of a mouse model for the study of Toscana virus pathogenesis. Virol 2005, 333:66–73
9. Meegan JM, Watten RH, Laughlin LH: Clinical experience with Rift Valley fever in humans during the 1977 Egyptian epizootic. Contrib Epidemiol Biostat 1981, 3:114–123
10. LeDuc JW, Cuevas M, Garcia M: The incidence and prevalence of phlebotomus fever group viruses in Panama. International Symposium on Tropical Arboviruses and Haemorrhagic Fevers. Belem, Brazil, 1980, pp. 385–390
11. Anderson GW Jr, Slayter M, Hall W, Peters CJ: Pathogenesis of a phleboviral infection (Punta Toro virus) in golden Syrian hamsters. Arch Virol 1990, 114:203–212
12. Yu H, Bauer B, Lipke GK, Phillips RL, Van Zant G. Apoptosis and hematopoiesis in murine fetal liver. Blood 1993, 81:373–384
13. Kang JI, Park SH, Lee PW, Ahn BY: Apoptosis is induced by hantaviruses in cultured cells. Virol 1999, 246:99–105
14. Markotic A, Hensley L, Geisbert T, Spik K, Schmaljohn C: Hantaviruses induce cytopathic effects and apoptosis in continuous human embryonic kidney cells. J Gen Virol 2003, 84:2197–2202
15. Akhmatova NK, Yusupova RS, Khaiboullina SF, Sibiryak SV: Lymphocyte apoptosis during hemorrhagic fever with renal syndrome. Russ J Immunol 2003, 8:37–46
16. Li XD, Makela TP, Guo D, Soliymani R, Koistinen V, Vapalahti V, Vaheri A, Lankinen H: Hantavirus nucleocapsid protein interacts with the Fas-mediated apoptosis enhancer Daxx. J Gen Virol 2002, 83:759–766
17. Li XD, Kukkonen S, Vapalahti O, Plyusnin A, Lankinen H, Vaheri A: Tula hantavirus infection of Vero E6 cells induces apoptosis involving caspase 8 activation. J Gen Virol 2004, 85:3261–3268
18. Li XD, Lankinen H, Putkuri N, Vapalahti O, Vaheri A: Tula hantavirus triggers pro-apoptotic signals of ER stress in Vero E6 cells. Virol 2005, 333:180–189
19. Hay S, Kannourakis G: A time to kill: viral manipulation of the cell death program. J Gen Virol 2002, 83:1547–1564
20. Roulston A, Marcellus RC, Branton PE: Viruses and apoptosis. Annu Rev Microbiol 1999, 53:577–628
21. Grummer B, Bendfeldt S, Wagner B, Greiser-Wike I: Induction of the intrinsic apoptotic pathway in cells infected with cytopathic bovine virus diarrhea virus. Virus Res 2002, 90:143–153
22. Thongtan T, Panyim S, Smith DR: Apoptosis in dengue virus infected liver cell lines HepG2 and Hep3B. J Med Virol 2004, 72:436–444
23. Espinoza JC, Cortes-Gutierrez M, Kuznar J: Necrosis of infectious pancreatic necrosis virus (IPNV) infected cells rarely is preceded by apoptosis. Virus Res 2005, 109:133–138
24. Martin DA, Elkon KB: Mechanisms of apoptosis. Rheum Dis Clin N Am 2004, 30:441–454
25. Yang JS, Ramanathan MP, Muthumani K, Choo AY, Jin SH, Yu QC, Hwang DS, Choo DK, Lee MD, Dang K, Tang W, Kim JJ, Weiner DB: Induction of inflammation by West Nile virus capsid through the caspase-9 apoptotic pathway. Emerg Infect Dis 2002, 8:1379–1384
26. Cleary ML, Smith SD, Sklar J: Cloning and structural analysis of cDNAs for bcl-2 and a hybrid bcl-2/immunoglobulin transcript resulting from the t(14;18) translocation. Cell 1986, 47:19–28
27. Zong WX, Lindsten T, Ross AJ, MacGregor GR, Tompson CB: BH3-only proteins that bind pro-survival Bcl-2 family members fail to induce apoptosis in the absence of Bax and Bak. Genes Dev 2001, 15:1481–1486
28. Morgan DM: Tetrazolium (MTT) assay for cellular viability and activity. Methods Mol Biol 1998, 79:179–183